Identification of QTL and Underlying Genes for Root System Architecture associated with Nitrate Nutrition in Hexaploid Wheat

Running head: Wheat Root Nitrate Responsive QTL and Genes

Marcus Griffiths[1], Jonathan A. Atkinson[1], Laura-Jayne Gardiner[2], Ranjan Swarup[1], Michael P. Pound[3], Michael H. Wilson[1], Malcolm J. Bennett[1] & Darren M. Wells[1*]

[1]School of Biosciences, University of Nottingham, Sutton Bonington Campus, LE12 5RD, UK.

[2]IBM Research, Warrington, WA4 4AD, UK.

***Corresponding author:** darren.wells@nottingham.ac.uk

Abstract

The root system architecture (RSA) of a crop has a profound effect on the uptake of nutrients and consequently the potential yield. However, little is known about the genetic basis of RSA and resource adaptive responses in wheat (*Triticum aestivum* L.). Here, a high-throughput germination paper plant phenotyping system was used to identify seedling traits in a wheat doubled haploid mapping population, Savannah × Rialto. Significant genotypic and nitrate-N treatment variation was found across the population for seedling traits with distinct trait grouping for root size-related traits and root distribution-related traits. Quantitative trait locus (QTL) analysis identified a total of 59 seedling trait QTLs. Across two nitrate treatments, 27 root QTLs were specific to the nitrate treatment. Transcriptomic analyses for one of the QTLs on chromosome 2D found under low nitrate conditions was pursued revealing gene enrichment in N-related biological processes and 17 candidate up-regulated genes with possible involvement in a root angle response. Together, these findings provide genetic insight into root system architecture and plant adaptive responses to nitrate and provide targets that could help improve N capture in wheat.

Keywords: Doubled-haploid population, Nitrate, RNA-seq, Quantitative trait loci, Root system architecture, Triticum aestivum L. (wheat).

1 Introduction

Nitrogen (N) is an essential macronutrient for plant growth and development with agriculture greatly dependent on synthetic N fertilisers for enhancing productivity. Global demand for fertilisers is projected to rise by 1.5% each year reaching 201.7 million tonnes in 2020, over half of which (118.8 million tonnes) is for nitrate fertilizers (FAO, 2017). However, there are compelling economic and environmental reasons to reduce N fertiliser use in agriculture, particularly as the N fixing process is reliant on unsustainable fossil fuels (Dawson *et al*., 2008).

The availability of nutrients is spatially and temporally heterogeneous in the soil (Lark *et al*., 2004; Miller *et al*., 2007). Roots therefore need to forage for such resources. The spatial arrangement of the root system, called the root system architecture (RSA) (Hodge *et al*., 2009), has a profound effect on the uptake of nutrients and consequently the potential yield. Optimisation of the RSA could significantly improve the efficiency of resource acquisition and in turn increase the yield potential of the crop. An improvement in N use efficiency (NUE) by just 1% could reduce fertiliser losses and save ~$1.1 billion annually (Delogu *et al*., 1998; Kant *et al*., 2010).

Understanding the contribution of root traits to RSA and function is of central importance for improving crop productivity. Roots however are inherently challenging to study leading to the wide use of artificial growth systems for plant phenotyping as they are generally high-throughput, allow precise control of environmental parameters and are easy to replicate. These phenotyping systems have been key for generating root phenotypic data for association mapping and uncovering underlying genetic mechanisms (Ren *et al*., 2012; Clark *et al*., 2013; Atkinson *et al*., 2015; Zurek *et al*., 2015; Yang *et al*., 2020). Such seedling phenotyping approaches have uncovered QTL for root system architectural traits on chromosome regions that have also been found in field trials for related traits (Bai *et al*., 2013; Atkinson *et al*., 2015). Only a limited number of studies have directly compared seedling screens to mature root traits in the field and overall results have been inconsistent, which likely reflects the lack of environmental control in the field, that seedling studies focus on the seminal root system and not the crown root system, and that field approaches for RSA research is in need of further development (Watt *et al*., 2013; Rich *et al*., 2020).

For many cereal crops, understanding the genetic basis of RSA is complex due to the polyploid nature and large genome sizes. Therefore, quantitative trait loci (QTL) analyses have been very useful for precisely linking phenotypes to regions of a chromosome. With the development of high-throughput RNA sequencing technology (RNA-seq), identified QTL can now be further dissected to the gene level. Using RNA-seq, a substantial number of genes and novel transcripts have been identified in cereal crops including rice, sorghum, maize and wheat that are implicated in RSA control (Oono *et al*., 2013; Gelli *et al*., 2014; Akpinar *et al*., 2015; Yu *et al*., 2015). To our knowledge, there are no other studies that have identified genes related to nitrate response or root angle change in wheat. The uncovering of these genes and mechanisms are likely to be of agronomical importance as they can then be implemented in genomics-assisted breeding programs to improve N-uptake efficiency in crops.

The aim of this study was to identify root traits and genes that relate to N uptake and plasticity in wheat. To achieve this, a germination paper-based system was used to phenotype a wheat doubled haploid (DH) mapping population under two N regimes. The nitrate-N levels were changed to determine the seedling responses to high- and low-affinity transport relevant concentrations as would be experienced in the field. Here were present genomic regions and underlying genes that we propose may control root size and root distribution responses in wheat to nitrate.

2 Results

2.1 Phenotypic variation in a wheat doubled haploid population for seedling traits and nitrate effects

Seedlings for 92 lines of the S×R DH mapping population and parents were grown hydroponically in a controlled environment chamber under high and low nitrate treatments (Fig. 1). Roots and shoots of each seedling were individually imaged 10 days after germination resulting in 6924 images. The results of ANOVA indicated that the variance for the genotype effects for all investigated seedling traits were highly significant ($p < 0.001$) (Table S1). Across the wheat population many of the root size and root distribution traits were found to be nitrate treatment-dependent. Interestingly, no significant differences were observed across the population for total root length in response to the nitrate treatment, however the root class distribution between lateral ($p < 0.001$) and seminal ($p < 0.01$) root length was significantly affected with a G×N-treatment interaction ($p < 0.001$). In addition, seminal root angle traits and width-depth related traits had significant nitrate treatment effects ($p < 0.05$). The seedling traits measured were also highly heritable with heritability scores for root length and count traits between 0.78-0.97, root distribution traits between 0.4-0.97, root angle traits between 0.51-0.84 and shoot traits between 0.77-0.84 (Table S1).

2.2 Wheat root phenotypic traits segregate into two distinct clusters by size and distribution

For the S×R DH population and parents a principal component analysis (PCA) was conducted to explore relationships within the root phenotypic traits (Fig. 2A). N treatment did not affect the PCA trait loadings or correlations between the traits (Fig. S1) so the analyses were conducted with both treatments together. Over 71% of the trait variation could be explained by the first two principal components and 90% of the trait variation could be explained by the first six principal components. The loadings were mostly split between root size related traits and root distribution traits (Fig. 2A). A correlation matrix of the whole dataset demonstrated the strong correlation between root size related traits and root distribution related traits (Fig. 2B). Of all the plant traits measured, the width-depth ratio traits were found to be positively correlated with the greatest number of traits from both trait groups, plant size and root distribution. In addition, the correlation analysis also highlighted negative associations between root size and angle traits.

2.3 Identification of novel root QTLs in the S×R DH population

Using normalized phenotypic data with a high-density Savannah × Rialto iSelect map, a total of 59 QTLs were discovered for seedling traits of which 41 QTLs had positive effect alleles that came from Savannah, and 18 from Rialto (Fig. 3, Table 2). QTLs were found on chromosomes 1A, 1B, 2D, 3B, 4D, 6D, 7A and 7D, with 25 QTLs located on 6D. For the rooting traits a total of 55 QTLs were found across two nitrate treatments, 23 of which were identified under the low nitrate treatment and 32 for the high nitrate treatment. Nine root QTLs were found to be only present in the low nitrate treatment, 18 root QTLs were found only in the high nitrate treatment and 14 root QTLs (28 total) were present in both nitrate treatments. The trait ANOVA results also support the root QTLs found are nitrate condition dependent. Phenotypic variation explained by QTLs varied from 3.8 to 82.9%. Of the QTLs found, there appear to be 13 underlying root QTLs, as many root size and root distribution class traits co-localized at the same chromosome region. Two QTLs involved in shoot size traits, which were identified on chromosomes 6D and 7D under low N, were colocalized with the corresponding QTLs of root size traits. N-dependent QTLs of some traits on chromosomes 6D and 7D were colocalized with N-independent QTLs of other root size traits. For QTLs associated with nitrate treatment, QTLs for root size were found on chromosomes 1A, 6D and 7D and for root angle on chromosomes 2D, 3B and 4D. Of these regions a candidate root angle QTL (RAE1001) residing on chromosome 2D was taken forward. For this QTL, a positive allele from Rialto conferred a root angle change in the low nitrate treatment that co-localised with other root angle traits and explained 14.3% of phenotypic variation with a small peak confidence region (25 cM) (Table 2).

2.4 Differentially regulated candidate genes for a root angle QTL identified by RNA-seq analysis

The lines selected for the RNA-seq analysis were based on the largest observed phenotypic differences for the trait associated with a root angle QTL located on chromosome 2D (RAE1001), found under low nitrate conditions. The DH population showed transgressive segregation with trait values more extreme than the parents (Fig. 4A). Under low nitrate there was a 30° difference in root angle ($p < 0.001$) between the extremes of the population with four lines of each taken forward for RNA-seq (Fig. 4B and C). The samples groups were also different for response to N with a significantly steeper root angle under low-nitrate in one of the groups ($p < 0.05$) (Fig. 4B).

One sample group was comprised of lines that had the candidate QTL with a positive effect from the parent Rialto (Group A: lines 17, 20, 36, 68) and the second sample group with parental origin from Savannah (Group B: lines 6, 8, 11, 52). As there was no single clear enriched region for the root QTL located on chromosome 2D, the whole chromosome was considered for differential gene expression analysis. A total of 3299 differentially expressed genes were identified in the analysed groups. We then focused on the identification of genes that were consistently overexpressed in Group A compared to Group B that could be driving the QTL. 1857 differentially expressed genes showed significant ($q < 0.05$) up-regulation in Group A (with the QTL) compared to Group B (without QTL) considering all four biological replicates in each case. Of these, 88 gene candidates resided on chromosome 2D. Additionally, MaSuRcA transcript assemblies were considered that were identified as significantly ($q < 0.05$) up-regulated in Group A compared Group B on chromosome 2D bringing the total to 93 (88 plus five) differentially expressed candidate sequences (Table S2). The inclusion of *de novo* assembled transcript sequences in the analysis factors for varietal specific genes that are not present in the Chinese Spring reference sequences. The sequencing read depth and alignment statistics are provided in Table S3. Of the 93 differentially expressed candidate sequences in Table S2, 17 candidate genes were consistently expressed across the Group A replicates verses zero reads mapping in one or more Group B replicates and were therefore considered as our primary candidates (Table 3). There were also 1442 differentially expressed genes that showed significant ($q < 0.05$) down-regulation in Group A (with the QTL) compared to Group B (without QTL). Of these, 65 were annotated as residing on chromosome 2D (Table S2).

Functional categories for the significantly up- and down-regulated genes were evaluated using g:profiler between contrasting sample groups for a root QTL found under low nitrate conditions. For terms relating to biological processes there were 58 up-regulated terms that had the same lowest *p*-value including "nitrogen compound metabolic process", "cellular nitrogen compound metabolic process", "regulation of nitrogen compound metabolic process" and "cellular nitrogen compound biosynthetic process" (Fig. 5). For the down-regulated terms, three of the top 10 terms included “nitrogen compound metabolic process”, “organonitrogen compound metabolic process” and “cellular nitrogen compound metabolic process” (Fig. 5). The complete list of enriched GO terms for molecular function, biological process and cellular component are available in Table S4. For the candidate root angle QTL found under low nitrate conditions (RAE1001) there were several N-related biological processes up- and down-regulated between the sample groups. In addition, within the candidate gene list an up-regulated NPF family gene, TraesCS2D02G348400, was identified which was consistently expressed across Group A and zero reads mapping in Group B. As this gene was expressed at low nitrate and within the identified QTL interval, *BS00010393–BS00066132_51*, the function of this gene was pursued. A phylogenetic analysis of protein families was conducted comparing NPF family protein sequences of *A. thaliana*, *O. sativa* and *T. aestivum* (Fig. S2). A total of 53 *A. thaliana* proteins, 130 *O. sativa* proteins and 391 *T. aestivum* proteins were aligned using MUSCLE with 1000 bootstrap interactions and 20 maximum likelihood searches (Edgar, 2004). The candidate *T. aestivum* protein TraesCS2D02G348400 is situated in a monocot specific sub-clade within the NPF4 clade (Fig. 6). This clade includes *A. thaliana* NPF members AtNPF4.1, AtNPF4.2, AtNPF4.3, AtNPF4.4, AtNPF4.5, AtNPF4.6 and AtNPF4.7. In addition, the candidate protein is closely related to a rice nitrate(chlorate)/proton symporter protein LOC_Os04g41410.

3 Discussion

Root system architecture is an important agronomic trait as the growth, development and spatial distribution of the root system affects the availability of soil resources that a plant can capture. Roots are challenging to phenotype in soil however without disturbing the spatial arrangement and therefore non-destructive root phenotyping systems such as germination paper screens and X-ray CT are invaluable tools for such work (Bai *et al*., 2013; Atkinson *et al*., 2015; Mooney *et al*., 2012). In this study a germination paper-based system was used to phenotype a wheat doubled haploid (DH) mapping population under two nitrate-N regimes as it is a suitable approach for population-size root phenotyping with precise nutrition control.

Within the Savannah × Rialto DH mapping population, significant genotypic and nitrate treatment dependent phenotypic variation was observed in seedling traits (Table S1). Overall, the seedling traits could be separated into two main groups of related traits which were for root size and root distribution. In the root size trait group, it was found that the population had significant nitrate responsive plasticity in root length distribution. Interestingly the root class length of seminal and lateral roots was significantly affected by nitrate treatment, yet overall, the total root length was not significantly different. The root distribution-related traits group appeared to be the most responsive to nitrate treatment in this physiological screen using the S×R DH mapping population. Both root length distribution and root angle are widely regarded as important traits that when plastic to abiotic stimuli, such as low N or drought, as a plant can change the root foraging distribution in the soil to find such resources (Ho *et al*., 2005; Trachsel *et al*., 2013).

Using high-throughput methods for growth and phenotyping enabled a whole wheat DH population to be scored for root and shoot traits and the data mapped to underlying chromosome regions by QTL analysis. Nitrate plasticity is a likely a component of these QTLs where they were only detected in one of the nitrate treatments. In addition, four QTLs were found for shoot size traits on chromosomes 6D and 7D in the low nitrate conditions (LOD > 2.0) (Fig. 3, Table 2). In the literature, there are also studies that have described QTL on regions associated with those found in this study for root and shoot seedling traits. In this study on chromosome 1A, it was found that the region is associated with lateral root traits under low nitrate conditions. Interestingly, chromosome 1A has been previously associated with lateral root length in wheat and rice (Ren *et al*., 2012; Beyer *et al*., 2018). Therefore, there are likely underlying genes on chromosome 1A which relate to resource foraging as they were found to affect root plasticity, tolerance and/or lateral root development increase grain yield in low input agricultural systems (An *et al*., 2006; Landjeva *et al*., 2008; Ren *et al*., 2012; Good *et al*., 2017; Guo *et al*., 2012; Zhang *et al*., 2013; Liu *et al*., 2013; Sun *et al*., 2013). This chromosome 1A region has also been correlated to nitrate uptake in S×R DH field trials (Atkinson *et al*., 2015) which would make this co-localized chromosome region an important candidate for further study with potential association between root traits and N uptake. In this study, root angle QTLs were also identified in the low nitrate conditions on chromosomes 2D, 3B and 4D. QTLs on these chromosomes have been described in other studies yet very few of these have measured root angle or distribution traits. From comparison with other studies that found root QTLs on chromosome 2D, it appears there may be an underlying gene or number of genes for seminal root development and/or plasticity (An *et al*., 2006; Zhang *et al*., 2013; Liu *et al*., 2013). On chromosome 3B, other studies have found QTLs affecting root size and stress related traits or genes relating to N plasticity, uptake and mobilisation (An *et al*., 2006; Habash *et al*., 2007; Guo *et al*., 2012; Zhang *et al*., 2013; Bai *et al*., 2013). On chromosome 4D, other studies have also found QTLs on this chromosome that indicates an underlying root development and/or root plasticity gene that may be affecting the root angle or distribution change (Zhang *et al*., 2013; Bai *et al*., 2013).

A seminal root angle QTL (LOD 3.0) on chromosome 2D found under low nitrate conditions was targeted for transcriptomic analysis. Significant GO enrichment in N-related biological processes were found in the chromosome region of lines with the QTL compared to those without indicating a differential low nitrate response in these lines. A total of 17 candidate up-regulated genes were identified that resided on chromosome 2D (Table 3). A more detailed list of the genes identified are given in Table S2. Two of the three genes with highest log changes plus four others have unknown function. Point mutation detection and mutant generation with TILLING or RNAi represent the next step to functionally characterise these genes. A promising candidate from the root transcriptomic analyses was an up-regulated nitrate transporter 1/peptide transporter (NPF) family gene NPF4 (TraesCS2D02G348400) in lines that had the root angle QTL. In *A. thaliana* and *O. sativa*, NPF family genes have important roles in lateral root initiation, branching and response to nitrate (Remans *et al*., 2006; Krouk *et al*., 2010; Fang *et al*., 2013). However, no studies have reported genes controlling root angle change in wheat, to date. A phylogenetic analysis of protein families was conducted comparing the protein sequences of *A. thaliana*, *O. sativa* and *T. aestivum* to the candidate protein. The candidate *T. aestivum* protein is situated in a monocot specific sub-clade within the NPF4 clade and is closely related to a rice nitrate(chlorate)/proton symporter protein (LOC_Os04g41410) (Fig. 6). Members of this clade are known for transporting the plant hormone abscisic acid (ABA) (AtNPF4.1 and AtNPF4.6) and have been demonstrated to have low affinity nitrate transport activity (AtNPF4.6) (Huang *et al*., 1999; Kanno *et al*., 2012). ABA is known to be a key regulator in root hydrotropism, a process that senses and drives differential growth towards

preferential water potential gradients (Antoni *et al*., 2016; Takahashi *et al*., 2002). As root angle is a determinant of root depth, pursuing this gene function is of agronomic importance for improving foraging capacity and uptake of nitrate in deep soil layers as seedling stage identified genes have been associated with yield-related traits (Xu *et al*., 2018).

In summary, we identified 59 QTLs using a wheat seedling hydroponic system, 27 of which were for root traits found in nitrate treatment specific conditions, 14 (28 total) for root QTLs found in both treatments, and four QTLs for shoot size traits. Using transcriptome analyses we found gene enrichment in N-related biological processes which may form part of a nitrate treatment developmental response affecting root angle. These findings provide a genetic insight into plant N adaptive responses and provide targets that could help improve N capture in wheat.

4 Materials and methods

4.1 Plant materials

A winter wheat doubled haploid mapping population comprised of 94 lines was used for root phenotyping. The population was derived from an F_1 plant between cultivars Savannah and Rialto (Limagrain UK Ltd, Rothwell, UK). Both parents are UK winter wheat cultivars that were on the AHDB recommended list. Savannah is a National Association of British & Irish Millers (nabim) Group 4 feed cultivar first released in 1998. Rialto is nabim Group 2 bread-making cultivar first released in 1995. Previous field research had found that Rialto had differential grain yield in low N field trials compared to Savannah making it a promising population to characterize with limited root characterization in response to N (Gaju *et al*., 2011).

4.2 Seedling phenotyping

Wheat seedlings were grown hydroponically using the system described in Atkinson *et al.* (2015) (Fig. 1). Seeds from the Savannah × Rialto doubled haploid (S×R DH) mapping population were sieved to a seed size range of 2.8–3.35 mm based on mean parental seed size. Seeds were surface sterilised in 5% (v/v) sodium hypochlorite for 12 minutes before three washes in dH2O. Sterilised seeds were laid on wet germination paper (Anchor Paper Company, St Paul, MN, USA) and stratified at 4°C in a dark controlled environment room for 5 days. After stratification seeds were transferred to a controlled environment room at 20/15°C, 12-hour photoperiod, 400 µmol m^{-2} s^{-1} PAR and kept in a light-tight container. After 48 hours, uniformly germinated seedlings with ~5 mm radicle length were transferred to vertically orientated seedling pouches.

Seeds for 94 lines from the S×R DH mapping population were grown hydroponically either in high nitrate (3.13 mM NO_3^-, 0.75 mM NH_4^+) or low nitrate (0.23 mM NO_3^-, 0.75 mM NH_4^+) modified Hoagland's solution (Table S5). The experimental design was a randomised block comprised of 94 genotypes split over 11 experimental runs with a target of 20 replications per genotype (n = 8 - 36). The RSA of each seedling was extracted from the images and stored in Root System Markup Language (RSML, Lobet *et al*., 2015) using the root tracing software RootNav (Pound *et al*., 2013). Root traits were quantified using RootNav standard functions and additional measurements as described in Atkinson *et al.* (2015). The shoot length and area were extracted from the shoot images using custom macros in the FIJI software package (Schindelin *et al*., 2012) (macro code available in Data S1). Definitions for all extracted traits are in Table 1. Analysis of variance of the raw plant data was conducted using R package "lmerTest" (Kuznetsova *et al*., 2017) with random effects by experimental run. Broad-sense heritability (h^2b) was calculated using the equation $h^2 = \sigma_g^2 / (\sigma_g^2 + \sigma_e^2)$ where σ_g^2 and σ_e^2 are the genetic and residual variances respectively (Falconer & Mackay, 1996). A principal component analysis (PCA) and correlation matrices were applied using R Stats Package v3.6.2 and "FactoMineR" (Husson *et al*., 2019) using the scaled mean values to explore the relationships between the traits and genotypes within the dataset. Finally, a correlation matrix was generated using R Statistics package "corrplot" (Wei & Simko, 2017) using the raw plant data from both treatments to determine overall correlations between traits.

4.3 Quantitative trait locus mapping

Detection of QTL and calculation of estimates for additive effects were conducted using the R Statistics package "R/qtl" (Broman *et al*., 2003). The map used was a high-density Savannah × Rialto iSelect map obtained from Wang *et al*. (2014) with redundant and closer than 0.5 cM markers stripped out reducing the number of effective markers from 46977 to 9239 markers. Average marker density by chromosome ranged between 0.16 and 4.23 markers per cM. Before QTL analysis, best linear unbiased predictions (BLUPs) were calculated for traits showing variance between experimental runs and best linear unbiased estimations (BLUEs) calculated for all other traits (Atkinson *et al.*, 2015; Henderson, 1975; Theil, 1970) (Data S2). QTL were identified based on the composite interval mapping (CIM) via extended Haley–Knott regression (Haley & Knott, 1992). The threshold logarithm of the odds (LOD) scores and effects were calculated by 1000 × permutation test at $p < 0.05$ level (Churchill & Doerge, 1994). After the analysis, an additional threshold was applied for

declaring presence of a QTL with a minimum LOD score of 2.0. The annotated linkage map was generated using R Statistics package "LinkageMapView" (Ouellette *et al*., 2018).

4.4 RNA-sequencing of candidate QTL

RNA-seq was used to identify underlying genes for a candidate seminal root angle QTL (LOD 3.0) located on chromosome 2D, found under low nitrate conditions. One sample group was comprised of lines that had the candidate QTL (Group A: lines 17, 20, 36, 68) and the second sample group did not have the QTL (Group B: lines 6, 8, 11, 52). All pooled root samples of plants grown under low nitrate were collected at the same time and immediately frozen using liquid nitrogen and stored at -80°C. Each sample group had four RNA biological replicates where each replicate was a pool of roots from three plants per line (12 plants per RNA sample). Total RNA was isolated from 500–1000 mg of homogenised root tissue (TRIzol reagent). RNA quality and purity were determined using a NanoDrop™ 2000c with values above 500 ng μL^{-1} or higher accepted. Illumina 75bp Paired-End Multiplexed RNA sequencing was performed using a using NextSeq 500 by Source Bioscience (Nottingham, UK).

Differential gene expression analysis was conducted using the IWGSC RefSeq v1.1 assembly (International Wheat Genome Sequencing Consortium, 2018) (http://plants.ensembl.org/Triticum_aestivum/) and the TGAC v1 Chinese Spring reference sequence (Clavijo *et al*., 2017). Raw sequencing reads were trimmed for adapter sequence and for regions where the average quality per base dropped below 15 (Trimmomatic version 0.32) (Bolger *et al*., 2014). After trimming, reads below 40 bp were eliminated from the dataset. Trimmed reads were aligned to the reference sequences assembly using splice-aware aligner HISAT2 (Pertea *et al*., 2016). Uniquely mapped reads were selected, and duplicate reads filtered out. Unmapped reads across all samples were assembled into transcripts using MaSuRCA software and sequences 250 bp or larger taken forward (Zimin *et al*., 2013). Unmapped reads were re-aligned to these assembled transcripts individually and added to their sample specific reads while the assembled transcripts were combined with the reference sequence and GTF annotation for downstream investigations. StringTie software was used to calculate gene and transcript abundances for each sample across the analysis specific annotated genes (Pertea *et al*., 2016). The sequencing read depth and alignment statistics are provided in Table S3. Finally, DEseq was used to visualise results and identify differential expression between samples (Anders & Huber, 2010). Differentially expressed genes were compared between the IWGSC RefSeq v1.1 and TGAC v1 reference assemblies to identify overlap using BLAST (BLASTN, e-value 1e-05, identity 95%, minimum length 40bp) (Altschul *et al*., 1990). The top matches for each gene between the reference sequences were used to allow an integrative and comprehensive annotation of genes. Gene ontology (GO) analysis was performed with the latest genome for *T. aestivum* (IWGSC RefSeq v1.1 assembly) in g:Profiler (Reimand *et al*., 2016) using the tailor made algorithm g:SCS for computing multiple testing correction for p-values gained from the GO enrichment analysis. A p-value threshold of 0.05 was applied with only results passing this threshold reported.

4.5 Phylogenetic analysis

A phylogenetic analysis of protein families was conducted to compare the protein sequences of *A. thaliana*, *O. sativa L.* and *T. aestivum L.* proton-dependent oligopeptide transporter (NPF) families (also known as the NRT1/PTR family). *A. thaliana* sequences were obtained from (Léran *et al*., 2014). Using the latest genome for *T. aestivum* (IWGSC RefSeq v1.1 assembly) and *O. sativa* (MSU Release 7.0, Kawahara *et al*., 2013, https://phytozome.jgi.doe.gov/) a HMM profile search was conducted (Krogh *et al*., 2001). The resulting list of proteins were scanned using Pfam (El-Gebali *et al*., 2019). Only single gene models of candidate genes with PTR2 domains were retained. The protein sequences were used to generate a maximum-likelihood tree using the software RAxML (Stamatakis, 2014). The exported tree file (.NWK) was then visualised using the R package "ggtree" (Yu *et al*., 2017) and used for phylogenetic tree construction. The exported tree file (.NWK) was visualised using the R package "ggtree" (Yu *et al*., 2017).

5 Data availability statement

The RNA-seq dataset is available (study PRJEB40436) from the European Nucleotide Archive (http://www.ebi.ac.uk/ena/data/view/PRJEB40436).

6 Funding

This work was supported by the Biotechnology and Biological Sciences Research Council [grant number BB/M001806/1, BB/L026848/1, BB/P026834/1] (MJB, DMW, and MPP); the Leverhulme Trust [grant number RPG-2016-409] (MJB and DMW); the European Research Council FUTUREROOTS Advanced Investigator grant [grant number 294729] to MG, JAA, DMW, and MJB; and the University of Nottingham Future Food Beacon of Excellence.

7 Disclosures

Conflicts of interest: No conflicts of interest declared

8 Acknowledgments

The authors would like to thank Limagrain UK Ltd for the use of the S×R DH population and Luzie U. Wingen (John Innes Centre) for providing rQTL scripts used in this work.

9 References

Akpinar B A, Kantar M, and Budak H. (2015) Root precursors of microRNAs in wild emmer and modern wheats show major differences in response to drought stress. *Funct Integr Genomics*. **15**, 587–598.

An D, Su J, Liu Q, Zhu Y, Tong Y, Li J, et al. (2006) Mapping QTLs for nitrogen uptake in relation to the early growth of wheat (Triticum aestivum L.). *Plant Soil*. **284**, 73–84.

Atkinson J A, Wingen, L U, Griffiths M, Pound M P, Gaju O, Foulkes M J, et al. (2015) Phenotyping pipeline reveals major seedling root growth QTL in hexaploid wheat. *J Exp Bot*. 66, 2283–2292.

Bai C, Liang Y, and Hawkesford M J. (2013) Identification of QTLs associated with seedling root traits and their correlation with plant height in wheat. *J Exp Bot*. 64, 1745–1753.

Beyer S, Daba S, Tyagi P, Bockelman H, Brown-Guedira G, and Mohammadi M. (2019) Loci and candidate genes controlling root traits in wheat seedlings—a wheat root GWAS. *Funct Integr Genomics*. 19, 91–107.

Bolger A M, Lohse M, and Usadel B. (2014) Trimmomatic: A flexible trimmer for Illumina sequence data. *Bioinformatics*. 30, 2114–2120.

Broman K W, Wu H, Sen Ś, and Churchill G A. (2003) R/qtl: QTL mapping in experimental crosses. *Bioinformatics*. 19, 889–890.

Churchill G A, and Doerge R W. (1994) Empirical threshold values for quantitative trait mapping. *Genetics*. 138, 963–971.

Clark R T, Famoso A N, Zhao K, Shaff J E, Craft E J, Bustamante C D, et al. (2013) High-throughput two-dimensional root system phenotyping platform facilitates genetic analysis of root growth and development. *Plant, Cell Environ*. 36, 454–466.

Dawson J C, Huggins D R, and Jones S S. (2008) Characterizing nitrogen use efficiency in natural and agricultural ecosystems to improve the performance of cereal crops in low-input and organic agricultural systems. *F Crop Res*. 107, 89–101.

Delogu G, Cattivelli L, Pecchioni N, De Falcis D, Maggiore T, and Stanca A M. (1998) Uptake and agronomic efficiency of nitrogen in winter barley and winter wheat. *Eur J Agron*. 9, 11–20.

Edgar R C. (2004) MUSCLE: Multiple sequence alignment with high accuracy and high throughput. *Nucleic Acids Res*. 32, 1792–1797.

El-Gebali S, Mistry J, Bateman A, Eddy S R, Luciani A, Potter S C, et al. (2019) The Pfam protein families database in 2019. *Nucleic Acids Res*. 47, D427–D432.

Falconer D S. (1996) Introduction to Quantitative Genetics (Fourth Edition), 4th Editio. ed. Longman Group Ltd., London.

Fang Z, Xia K, Yang X, Grotemeyer M S, Meier S, Rentsch D, et al. (2013) Altered expression of the PTR/NRT1 homologue OsPTR9 affects nitrogen utilization efficiency, growth and grain yield in rice. *Plant Biotechnol J*. 11, 446–458.

FAO. (2017). World fertilizer Trends and Outlook to 2020. Food and Agriculture Organization of the United Nations. Rome, Italy. Available online at: http://www.fao.org/3/a-i6895e.pdf (Accessed January 20, 2019).

Gaju O, Allard V, Martre P, Snape J W, Heumez E, LeGouis J, et al. (2011) Identification of traits to improve the nitrogen-use efficiency of wheat genotypes. *F Crop Res*. 123, 139–152.

Gelli M, Duo Y, Konda A R, Zhang C, Holding D, and Dweikat I. (2014) Identification of differentially expressed genes between sorghum genotypes with contrasting nitrogen stress tolerance by genome-wide transcriptional profiling. *BMC Genomics*. 15, 1–16.

Good A G, Johnson S J, De Pauw M, Carroll R T, Savidov N, Vidmar J, et al. (2007) Engineering nitrogen use efficiency with alanine aminotransferase. *Can J Bot*. 85, 252–262.

Guo Y, Kong F mei, Xu Y feng, Zhao Y, Liang X, Wang Y ying, et al. (2012) QTL mapping for seedling traits in wheat grown under varying concentrations of N, P and K nutrients. *Theor Appl Genet*. 124, 851–865.

Habash, D.Z., Bernard, S., Schondelmaier, J., Weyen, J., and Quarrie, S.A. (2007) The genetics of nitrogen use in hexaploid wheat: N utilisation, development and yield. *Theor Appl Genet*. 114, 403–419.

Haley C S, and Knott S A. (1992) A simple regression method for mapping quantitative trait loci in line crosses using flanking markers. *Heredity*. 69, 315–324.

Henderson C R. (1975). Best Linear Unbiased Estimation and Prediction under a Selection Model. *Biometrics*. 31, 423–44.

Ho C H, Lin S H, Hu H C, and Tsay Y F. (2009) CHL1 Functions as a Nitrate Sensor in Plants. *Cell*. 138, 1184–1194.

Hodge A, Berta G, Doussan C, Merchan F, and Crespi M. (2009) Plant root growth, architecture and function, *Plant and Soil*. 321, 153-187.

Huang N C, Liu K H, Lo H J, and Tsay Y F. (1999) Cloning and functional characterization of an Arabidopsis nitrate transporter gene that encodes a constitutive component of low-affinity uptake. *Plant Cell*. 11, 1381–1392.

Husson F, Josse J, Le S, and Maintainer J M. (2019) R Package "FactoMineR": Multivariate exploratory data analysis and data mining [WWW Document]. URL https://github.com/husson/FactoMineR

International Wheat Genome Sequencing Consortium. (2018) Shifting the limits in wheat research and breeding using a fully annotated reference genome. *Science*. 361.

Kanno Y, Hanada A, Chiba Y, Ichikawa T, Nakazawa M, Matsui M, et al. (2012) Identification of an abscisic acid transporter by functional screening using the receptor complex as a sensor. *Proc Natl Acad Sci USA*. 109, 9653–9658.

Kant S, Bi Y M, and Rothstein S J. (2011) Understanding plant response to nitrogen limitation for the improvement of crop nitrogen use efficiency. *J Exp Bot*. 62, 1499–1509.

Kawahara Y, de la Bastide M, Hamilton J P, Kanamori H, Mccombie W R, Ouyang S, et al. (2013) Improvement of the oryza sativa nipponbare reference genome using next generation sequence and optical map data. *Rice*. 6, 3–10.

Krogh A, Larsson B, Von Heijne G, and Sonnhammer E L L. (2001) Predicting transmembrane protein topology with a hidden Markov model: Application to complete genomes. *J Mol Biol*. 305, 567–580.

Krouk G, Lacombe B, Bielach A, Perrine-Walker F, Malinska K, Mounier E, et al. (2010) Nitrate-regulated auxin transport by NRT1.1 defines a mechanism for nutrient sensing in plants. *Dev Cell*. 18, 927–937.

Kuznetsova A, Brockhoff P B, Christensen R H B. (2017). lmerTest Package: Tests in Linear Mixed Effects Models. *J Stat Softw*. 82.

Landjeva S, Neumann K, Lohwasser U, and Börner A. (2008) Molecular mapping of genomic regions associated with wheat seedling growth under osmotic stress. *Biol Plant*. 52, 259–266.

Lark R M, Milne A E, Addiscott T M, Goulding K W T, Webster C P, O'Flaherty S. (2004). Scale- and location-dependent correlation of nitrous oxide emissions with soil properties: An analysis using wavelets. *Eur J Soil Sci*. 55, 611–627.

Léran S, Varala K, Boyer J C, Chiurazzi M, Crawford N, Daniel-Vedele F, et al. (2014) A unified nomenclature of nitrate transporter 1/peptide transporter family members in plants. *Trends Plant Sci*. 19, 5–9.

Liu X, Li R, Chang X, and Jing R. (2013) Mapping QTLs for seedling root traits in a doubled haploid wheat population under different water regimes. *Euphytica*. 189, 51–66.

Lobet G, Pound M P, Diener J, Pradal C, Draye X, Godin C, et al. (2015) Root system markup language: Toward a unified root architecture description language. *Plant Physiol*. 167, 617–627.

Miller A J, Fan X, Orsel M, Smith S J, Wells D M. (2007). Nitrate transport and signalling. *J Exp Bot*. 58, 2297–2306.

Mooney S J, Pridmore T P, Helliwell J, and Bennett M J. (2012) Developing X-ray computed tomography to non-invasively image 3-D root systems architecture in soil. *Plant Soil*. 352, 1–22.

Oono Y, Kawahara Y, Yazawa T, Kanamori H, Kuramata M, Yamagata H, et al. (2013) Diversity in the complexity of phosphate starvation transcriptomes among rice cultivars based on RNA-Seq profiles. *Plant Mol Biol*. 83, 523–537.

Ouellette L A, Reid R W, Blanchard S G, and Brouwer C R. (2018) LinkageMapView-rendering high-resolution linkage and QTL maps. *Bioinformatics*. 34, 306–307.

Pertea M, Kim D, Pertea G M, Leek J T, and Salzberg S L. (2016) RNA-seq experiments with HISAT , StringTie and Ballgown. *Nat Protoc*. 11, 1650–1667.

Pound M P, French A P, Atkinson J A, Wells D M, Bennett M J, and Pridmore T. (2013) RootNav: Navigating images of complex root architectures. *Plant Physiol*. 162, 1802–1814.

Raudvere U, Kolberg L, Kuzmin I, Arak T, Adler P, Peterson H, et al. (2019) G:Profiler: A web server for functional enrichment analysis and conversions of gene lists (2019 update). *Nucleic Acids Res*. 47, W191–W198.

Remans T, Nacry P, Pervent M, Filleur S, Diatloff E, Mounier E, et al. (2006) The Arabidopsis NRT1.1 transporter participates in the signaling pathway triggering root colonization of nitrate-rich patches. *Proc Natl Acad Sci USA*. 103, 19206–19211.

Ren Y, He X, Liu D, Li J, Zhao X, Li B, et al. (2012) Major quantitative trait loci for seminal root morphology of wheat seedlings. *Mol Breed*. 30, 139–148.

Rich S M, Christopher J, Richards R, Watt M. (2020). Root phenotypes of young wheat plants grown in controlled environments show inconsistent correlation with mature root traits in the field. *J Exp Bot*. 71, 4751–4762.

Schindelin J, Arganda-Carrera I, Frise E, Verena K, Mark L, Tobias P, et al. (2009) Fiji - an Open platform for biological image analysis. *Nat Methods*. 9.

Stamatakis A. (2014) RAxML version 8: A tool for phylogenetic analysis and post-analysis of large phylogenies. *Bioinformatics*. 30, 1312–1313.

Sun J jie, Guo Y, Zhang Gui zhi, Gao, M gang, Zhang Guo hua, Kong F. mei, et al. (2013) QTL mapping for seedling traits under different nitrogen forms in wheat. *Euphytica*. 191, 317–331.

Theil H. (1971). Best Linear Unbiased Estimation and Prediction. In: Principles of Econometrics. John Wiley & Sons, New York. 119–124.

Trachsel S, Kaeppler S M, Brown K M, and Lynch J P. (2013) Maize root growth angles become steeper under low N conditions. *F Crop Res*. 140, 18–31.

Wang S, Wong D, Forrest K, Allen A, Chao S, Huang B E, et al. (2014). Characterization of polyploid wheat genomic diversity using a high-density 90 000 single nucleotide polymorphism array. *Plant Biotechnol J*. 12, 787–796.

Watt M, Moosavi S, Cunningham S C, Kirkegaard J A, Rebetzke G J, Richards R A. (2013). A rapid, controlled-environment seedling root screen for wheat correlates well with rooting depths at vegetative, but not reproductive, stages at two field sites. *Ann Bot*. 112, 447–455.

Wei T, Simko V. (2017) R package 'corrplot': Visualization of a Correlation Matrix (Version 0.84) [WWW Document]. URL https://github.com/taiyun/corrplot (accessed 7.28.20).

Xu C, Zhang H, Sun J, Guo Z, Zou C, Li W X, et al. (2018) Genome-wide association study dissects yield components associated with low-phosphorus stress tolerance in maize. *Theor Appl Genet*. 131, 1699–1714.

Yang M, Wang C R, Hassan M A, Wu Y Y, Xia X. (2020) QTL mapping of seedling biomass and root traits under different nitrogen conditions in bread wheat (Triticum aestivum L .). *J Integr Agric*. 19, 2–14.

Yu G, Smith D K, Zhu H, Guan Y, and Lam T T Y. (2017) Ggtree: an R Package for Visualization and Annotation of Phylogenetic Trees With Their Covariates and Other Associated Data. *Methods Ecol Evol*. 8, 28–36.

Yu P, Eggert K, von Wirén N, Li C, and Hochholdinger F. (2015) Cell type-specific gene expression analyses by RNA sequencing reveal local high nitrate-triggered lateral root initiation in shoot-borne roots of maize by modulating auxin-related cell cycle regulation. *Plant Physiol*. 169, 690–704.

Zhang H, Cui F, Wang L, Li J, Ding A, Zhao C, et al. (2013) Conditional and unconditional QTL mapping of drought-tolerance-related traits of wheat seedling using two related RIL populations. *J Genet*. 92, 213–231.

Zimin A V, Marçais G, Puiu D, Roberts M, Salzberg S L, and Yorke J A. (2013) The MaSuRCA genome assembler. *Bioinformatics*. 29, 2669–2677.

Zurek P R, Topp C N, and Benfey P N. (2015) Quantitative trait locus mapping reveals regions of the maize genome controlling root system architecture. *Plant Physiol*. 167, 1487–1496.

10 Tables

Table 1. Definition of plant traits measured.

Acronym	Definition	Software	Units
RAE1	Angle of emergence between the outermost seminal roots measured at 30 px	RootNav	Degrees (°)
RAE1001	Angle of emergence between outermost pair of seminal roots measured at root tip	RootNav	Degrees (°)
RAE1002	Angle of emergence between innermost pair of seminal roots measured at root tip	RootNav	Degrees (°)
RAE2	Angle of emergence between innermost pair of seminal roots measured at 30 px	RootNav	Degrees (°)
RAE251	Angle of emergence between outermost pair of seminal roots measured at first quartile of total length	RootNav	Degrees (°)
RAE252	Angle of emergence between innermost pair of seminal roots measured at first quartile of total length	RootNav	Degrees (°)
RAE501	Angle of emergence between outermost pair of seminal roots measured at second quartile of total length	RootNav	Degrees (°)
RAE502	Angle of emergence between innermost pair of seminal roots measured at first quartile of total length	RootNav	Degrees (°)
RAE751	Angle of emergence between outermost pair of seminal roots measured at third quartile of total length	RootNav	Degrees (°)
RAE752	Angle of emergence between innermost pair of seminal roots measured at third quartile of total length	RootNav	Degrees (°)
RAE951	Angle of emergence between outermost pair of seminal roots measured at 95 px	RootNav	Degrees (°)
RAE952	Angle of emergence between innermost pair of seminal roots measured at 95 px	RootNav	Degrees (°)
RCH	Convex hull - area of the smallest convex polygon to enclose the root system	RootNav	mm2
RCHCX	Convex hull centroid - horizontal co-ordinate	RootNav	mm
RCHCY	Convex hull centroid - vertical co-ordinate	RootNav	mm
RCMX	Root centre of mass- horizontal co-ordinate	RootNav	mm
RCMY	Root centre of mass - vertical co-ordinate	RootNav	mm
RLC	Number of lateral roots	RootNav	Dimensionless (Count)
RMD	Maximum depth of the root system	RootNav	mm
RMW	Maximum width of the root system	RootNav	mm
RWDR	Width-depth ratio (MW/MD)	RootNav	Dimensionless (Ratio)
RSC	Number of seminal roots	RootNav	Dimensionless (Count)
RTLA	Total length of all roots	RootNav	mm
RTLL	Total length of lateral roots	RootNav	mm
RTLS	Total length of seminal roots	RootNav	mm
SA	Shoot area	FIJI	mm^2
SH	Shoot height	FIJI	mm

439 **Table 2**. QTLs for wheat seedling traits detected in the S×R DH population grown in hydroponics (LOD > 2.0). Trait
440 units as Table 1. Note: shoot data available for low nitrate conditions only.

Trait	Treat	QTL	Marker interval[a]	Site[b] (cM)	LOD[c]	Additive effect[d]	PVE[e] (%)
RTLA	LN	6D	BobWhite_c7090_522–BS00023964	5.0	27.4	-229	65.0
		7D	wsnp_Ku_c416_869895–BS00028760_51	26.0	8.4	-107	11.3
	HN	6D	BobWhite_c7090_522–BS00023964	4.4	23.0	-201	57.4
		7D	wsnp_Ku_c416_869895–BS00028760_51	27.0	8.7	-111	14.3
RTLS	LN	6D	BobWhite_c7090_522–BS00023964	5.0	33.5	-198	70.5
		7D	wsnp_Ku_c416_869895–BS00028760_51	26.0	11.3	-86	12.1
	HN	6D	BobWhite_c7090_522–BS00023964	4.4	24.8	-168	59.9
		7D	wsnp_Ku_c416_869895–BS00028760_51	27.0	9.4	-91.2	14.4
RTLL	LN	1A	BS00004043–BS00000226	215.0	2.3	-9.0	6.2
		6D	BobWhite_c7090_522–BS00023964	8.0	13.4	-31.2	48.0
	HN	6D	BS00009514–BS00023964	4.4	6.3	-32.8	28.0
RAE1	HN	3B	BobWhite_c22370_352–wsnp_RFL_Contig3336_3426054	178.8	2.2	-11.0	10.8
RAE2	HN	3B	GENE-1154_396–wsnp_RFL_Contig3336_3426054	178.8	2.8	-8.2	13.3
RLC	LN	1A	BS00004043–BS00000226	216.0	4.9	-2.4	8.6
		6D	BobWhite_c7090_522–BS00023964	5.0	19.6	-9.4	52.8
		7D	wsnp_Ku_c416_869895–BS00028760_51	22.0	6.0	-4.4	10.9
	HN	6D	BS00009514–BS00023964	4.4	8.8	-8.5	36.5
RSC	LN	6D	BS00009514–BS00022787	4.4	3.2	0.2	13.1
		7D	wsnp_Ku_c416_869895–IAAV4624	23.0	3.8	-0.2	15.8
	HN	7A	Excalibur_c48636_283–wsnp_RFL_Contig2864_2688208	12.0	2.9	0.2	13.7
RCH	LN	6D	BobWhite_c7090_522–BS00023964	4.4	31.1	-8464	80.0
	HN	6D	BobWhite_c7090_522–BS00023964	4.4	18.4	-7118	53.5
		7D	wsnp_Ku_c416_869895–Kukri_c46303_512	34.0	4.2	-3309	8.3
RMW	LN	1B	IAAV3905–wsnp_RFL_Contig3951_4390396	12.5	3.6	-8.9	5.0
		6D	BobWhite_c7090_522–BS00023964	4.4	26.7	-48.5	72.8
	HN	4D	wsnp_Ex_c9440_15657149–wsnp_Ku_c16354_25219645	23.9	3.1	10.8	7.1
		6D	BS00009514–BS00023964	4.4	16.4	-36.2	54.6
RMD	LN	6D	BobWhite_c7090_522–BS00023964	4.4	31.5	-71.4	75.1
		7D	wsnp_Ku_c416_869895–BS00021859	27.0	3.7	-20.6	3.8
	HN	6D	BobWhite_c7090_522–BS00023964	4.4	21.8	-60.3	58.8
		7D	wsnp_Ku_c416_869895–BS00028760_51	30.0	5.2	-26.6	8.6
RMWD	LN	1B	RAC875_c2185_1138–BobWhite_c23617_167	86.2	2.2	-0.03	10.5
	HN	4D	wsnp_Ex_c9440_15657149–BS00065168	4.8	3.1	0.1	14.6
RCMX	LN	6D	BS00009514–BS00023964	6.0	2.3	1.6	11.2
	HN	1A	GENE-0249_122–BS00075532_51	145.0	4.1	-1.7	16.6
		6D	BS00009514–BS00023964	22.0	4.0	1.5	16.3
RCMY	LN	6D	BobWhite_c7090_522–BS00023964	4.4	31.9	-23.1	80.8
	HN	6D	BobWhite_c7090_522–BS00023964	4.4	19.5	-19.3	63.5
RCHCX	LN	6D	BS00009514–BS00023964	4.4	2.3	2.5	11.2

	HN	6D	BS00009514–BS00023964	18.0	3.2	2.14	12.9
		7D	wsnp_Ku_c416_869895–IAAV4624	21.0	3.2	2.6	13.1
RCHCY	LN	6D	BobWhite_c7090_522–BS00023964	4.4	34.1	-40.0	82.9
	HN	3B	BS00064778–BS00075879	216.2	4.9	7.11	6.8
		6D	BobWhite_c7090_522–BS00023964	4.4	25.0	-33.9	62.1
		7D	wsnp_Ku_c416_869895–Kukri_c46303_512	32.0	5.8	-14.4	8.2
RAE951	HN	3B	RAC875_c5799_224–wsnp_Ra_c7158_12394405	178.8	2.8	-7.7	13.3
RAE251	HN	3B	BobWhite_c22370_352–wsnp_CAP11_c323_263800	178.8	3.6	-7.7	17.0
RAE252	HN	4D	wsnp_Ex_c9440_15657149–BS00065168	0.8	2.8	6.5	13.4
RAE501	HN	4D	wsnp_Ex_c9440_15657149–BS00065168	0.8	2.9	6.3	14.0
RAE502	HN	4D	wsnp_Ex_c9440_15657149–BS00065168	0.8	3.0	6.4	14.2
RAE751	LN	2D	BS00010393–BS00066132_51	160.0	2.6	5.1	12.5
	HN	4D	wsnp_Ex_c9440_15657149–BS00024014	0.8	2.9	6.3	13.8
RAE752	HN	4D	wsnp_Ex_c9440_15657149–BS00065168	0.8	2.1	5.3	10.4
RAE1001	LN	2D	BS00010393–BS00066132_51	160.0	3.0	5.5	14.3
	HN	4D	wsnp_Ex_c9440_15657149–BS00024014	0.8	2.4	6.0	11.9
SA	LN	6D	BobWhite_c7090_522–BS00023964	8.0	24.4	-1.0	61.4
		7D	wsnp_Ku_c416_869895–	29.0	7.0	-0.6	10.6
SH	LN	6D	BS00009514–BS00023964	4.4	19.3	-0.6	54.5
		7D	wsnp_Ku_c416_869895–Kukri_c46303_512	31.0	6.0	-0.3	11.7

[a] Chromosome region of the QTL defined by two flanking markers
[b] Genetic position of the QTL peak value
[c] Logarithm of the odds value
[d] Additive effects of putative QTL; a positive value indicates that positive alleles are from Rialto; negative values indicate positive alleles are from Savannah
[e] Percentage of phenotypic variation explained by putative QTL

448 **Table 3**. Candidate genes for seminal root angle QTL located on chromosome 2D that were consistently expressed across
449 the Group A replicates verses zero reads mapping in one or more Group B replicates. Gene naming convention according
450 to IWGSC RefSeq v1.1. Genes that are present on a chromosome that is not chromosome 2D represent variation between
451 the IWGSC RefSeqv1.1 and the TGACv1 assembly.

Gene	Log_2 fold change	Adjusted p value (q value)	Functional annotation
TraesCS2D02G088100	1.29	0.036	C2H2-type zinc finger
TraesCS2D02G108500	1.38	0.026	Peroxidase
TraesCS2D02G129100	1.36	0.036	Legume lectin domain
MSTRG.42598 (TGACv1)	1.31	0.041	Unknown
TraesCS2B02G126600	2.21	9.5E-06	Unknown
TraesCS6A02G175000	1.66	0.002	Nuclear pore complex scaffold, nucleoporin
TraesCS2D02G270000	1.66	0.002	Helix-loop-helix DNA-binding domain
TraesCS2D02G330200	1.44	0.013	Unknown
TraesCS2A02G111200	2.12	2.5E-05	Kelch motif
TraesCS2D02G344400	1.45	0.013	Unknown
TraesCS2D02G348400	1.88	3.6E-04	NPF4
MSTRG.40366 (TGACv1)	2.02	8.9E-05	Unknown
TraesCS4B02G057100	1.48	0.013	Unknown
TraesCS2D02G441300	1.29	0.037	AAA domain UvrD/REP helicase N-terminal domain
TraesCS2D02G487000	1.53	0.008	DUF wound-responsive family protein
TraesCS2D02G509700	1.73	0.002	Peroxidase
TraesCS2D02G511200	1.41	0.025	Peroxidase

452

11 Legends to Figures

Fig. 1. High-throughput hydroponic phenotyping system for seedling root & shoot traits. (A) Growth assembly and plant imaging station. (B) Example image of a wheat root grown on germination paper 10 days after germination. (C) Root system extraction to RSML database using RootNav software. (D) Measurement of root traits from RSML database. (E) Example image of a wheat shoot 10 days after germination. (F) Shoot image colour thresholding & shoot measurement using FIJI. (G) Example of QTL peak extracted from phenotyping data & mapping data with rQTL.

Fig. 2. (A) PCA ordination results for S×R doubled haploid population and parents under high and low nitrate regimes. Arrows indicate directions and contributions of loadings for each trait. (B) Correlation matrix of extracted root traits averaged between nitrate treatments. Correlations are colour coded from strong positive correlation in red to strong negative correlation in blue with no correlation shown in white.

Fig. 3. Molecular linkage map showing position of QTLs detected in the S×R DH population grown in hydroponics (LOD > 2.0). QTLs and confidence regions for all root traits are colour labelled by nitrate condition, low nitrate (blue), high nitrate (red) and nitrate treatment independent (green). Shoot QTLs found in the low nitrate study are shown in grey.

Fig. 3. Molecular linkage map showing position of QTLs detected in the S×R DH population grown in hydroponics (LOD > 2.0). QTLs and confidence regions for all root traits are colour labelled for low N-dependent (blue), high N-dependent (red) and N treatment independent (green). Shoot QTL found in low N study are shown in grey. Marker density (MD) per chromosome is displayed as average cM per 1 marker.

Fig. 4. (A) Distribution of means for seminal root angle (RAE1001) for S×R doubled haploid population under two nitrate regimes. Labelled non-parental lines were selected for RNA-seq. (B) Boxplot and (C) overlay plot for lines selected for RNA-seq with differential seminal root angle (RAE1001).

Fig. 5. GO enrichment analysis for top Biological process GO terms with the highest p-value for up- and down-regulated genes in the sample group with a candidate seminal root angle QTL compared to without the QTL.

Fig. 6. Phylogenetic tree of protein families comparing the protein sequences of A. thaliana, O. sativa L. and T. aestivum L. NPF family proteins to an identified candidate T. aestivum. protein. The candidate T. aestivum. protein is situated in a monocot specific outgroup within a NPF4 protein clade (highlighted in red). Branch lengths are proportional to substitution rate.

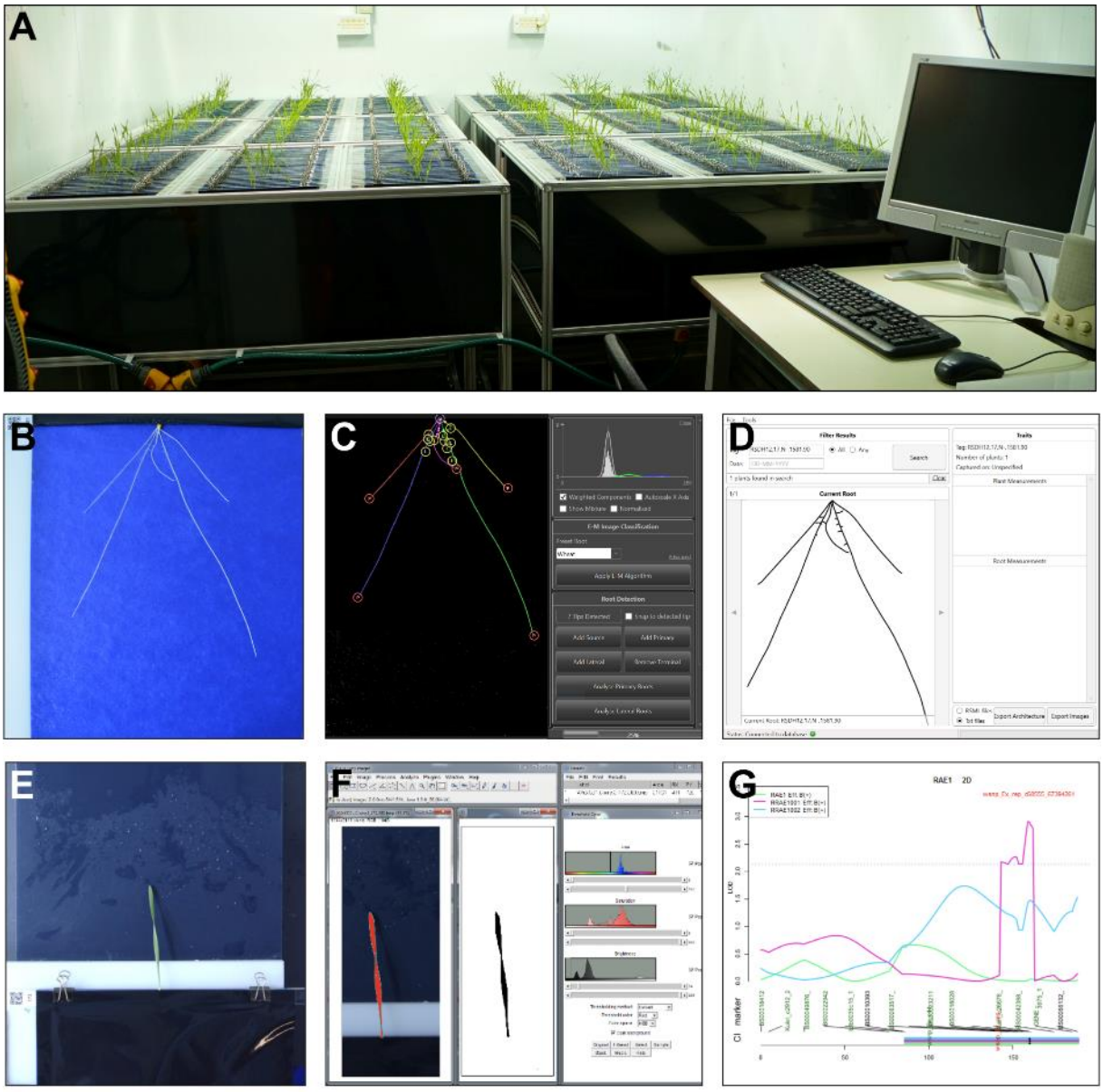

Figure 1. High-throughput hydroponic phenotyping system for seedling root & shoot traits. **(A)** Growth assembly and plant imaging station. **(B)** Example image of a wheat root grown on germination paper 10 DAG. **(C)** Root system extraction to RSML database using RootNav software. **(D)** Measurement of root traits from RSML database. **(E)** Example image of a wheat shoot 10 DAG. **(F)** Shoot image colour thresholding & shoot measurement using FIJI. **(G)** Example of QTL peak extracted from phenotyping data & mapping data with rQTL.

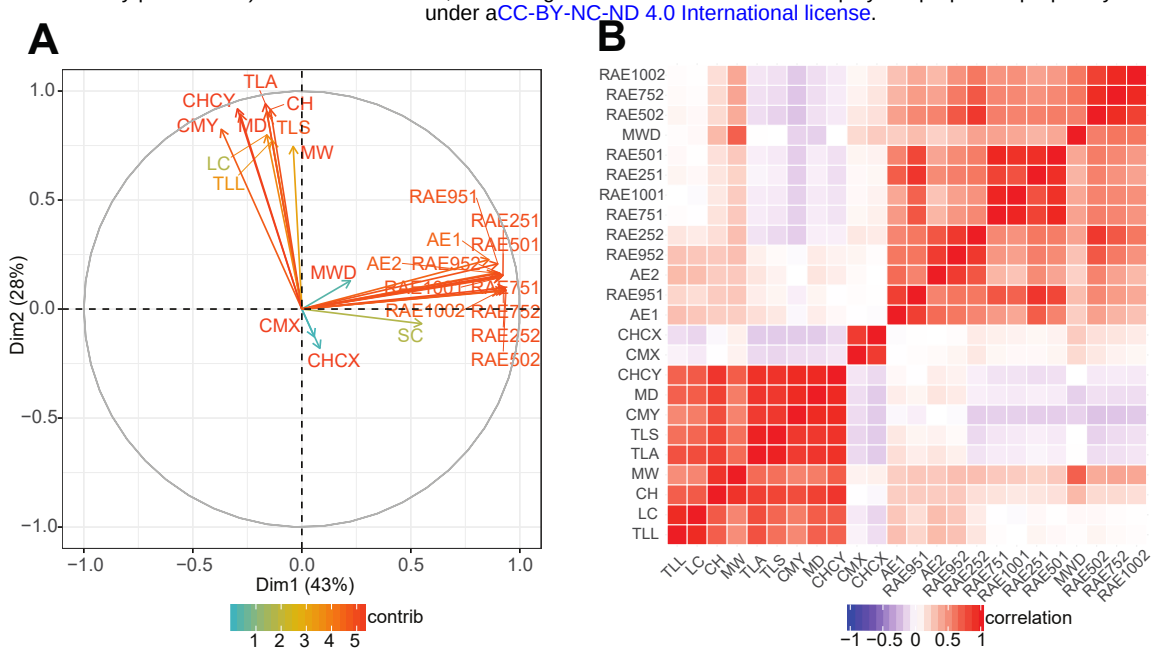

Figure 2. (A) PCA ordination results for S×R doubled haploid population and parents under high and low nitrate regimes. Arrows indicate directions and contributions of loadings for each trait. **(B)** Correlation matrix of extracted root traits averaged between nitrate treatments. Correlations are colour coded from strong positive correlation in red to strong negative correlation in blue with no correlation shown in white.

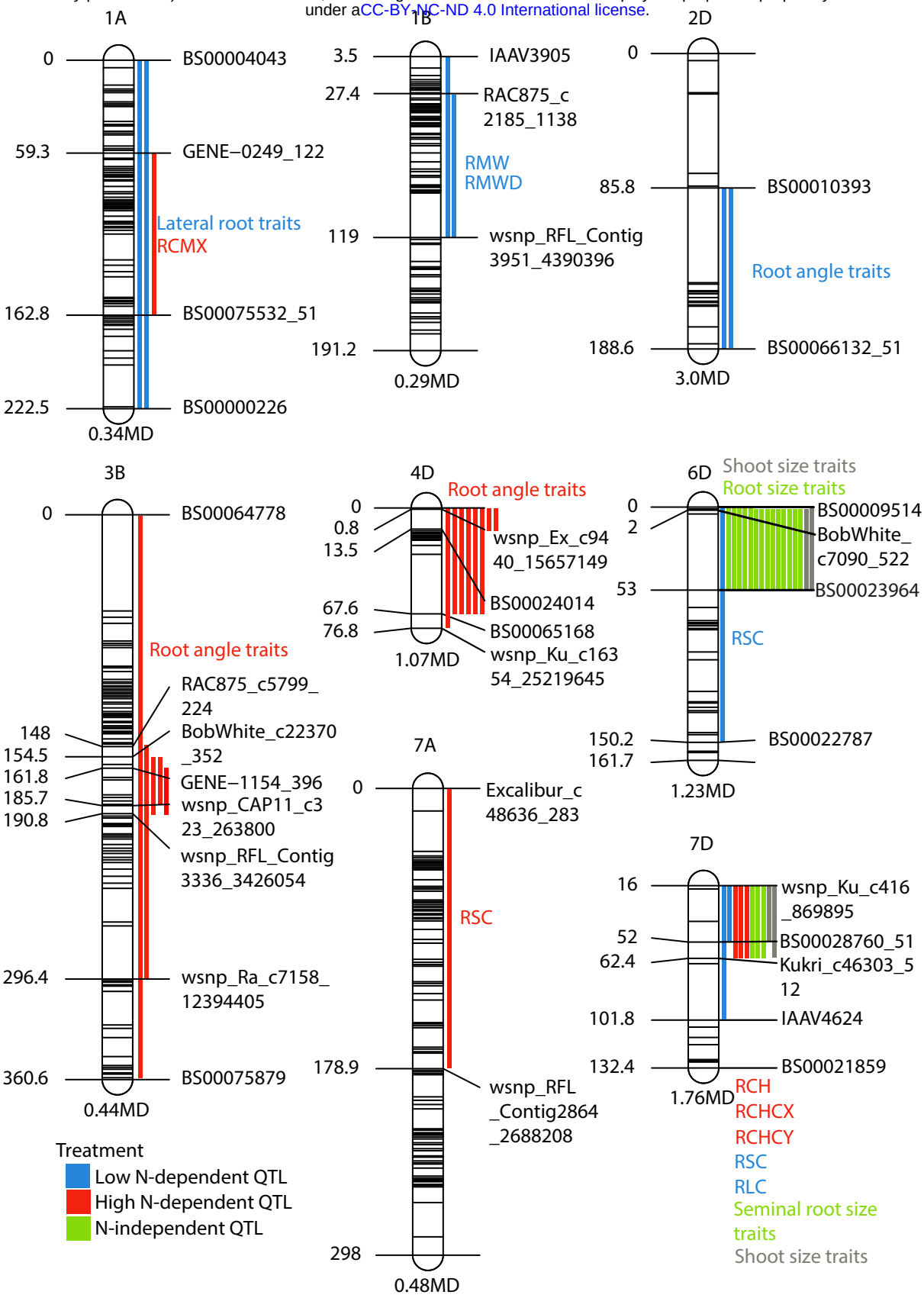

Figure 3. Molecular linkage map showing position of QTLs detected in the S×R DH population grown in hydroponics (LOD > 2.0). QTLs and confidence regions for all root traits are colour labelled by nitrate condition, low nitrate (blue), high nitrate (red) and nitrate treatment independent (green). Shoot QTLs found in the low nitrate study are shown in grey.

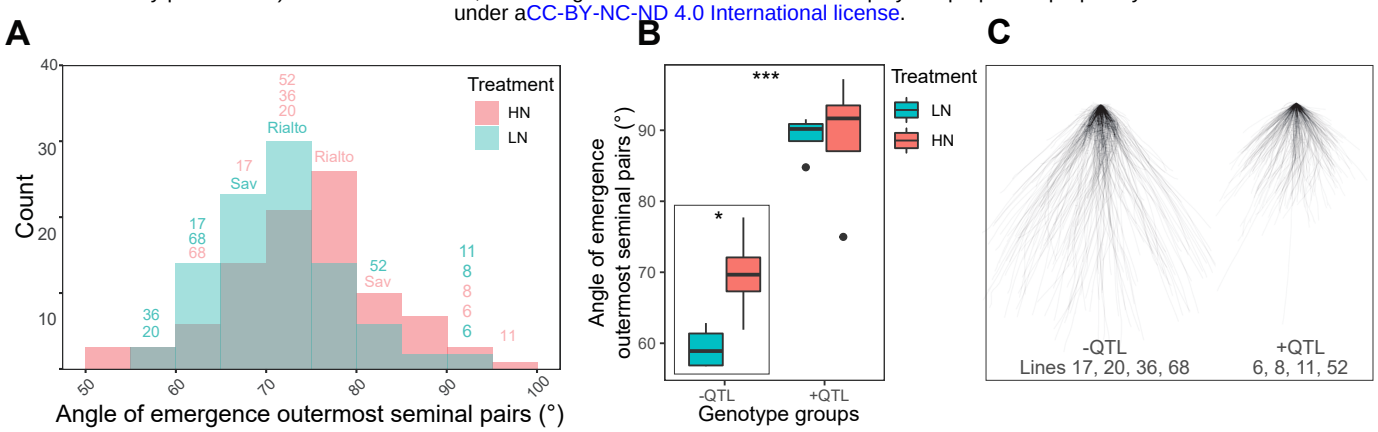

Figure 4. (A) Distribution of means for seminal root angle (RAE1001) for S×R doubled haploid population under two nitrate regimes. Labelled non-parental lines were selected for RNA-seq. **(B)** Boxplot and **(C)** overlay plot for lines selected for RNA-seq with differential seminal root angle (RAE1001).

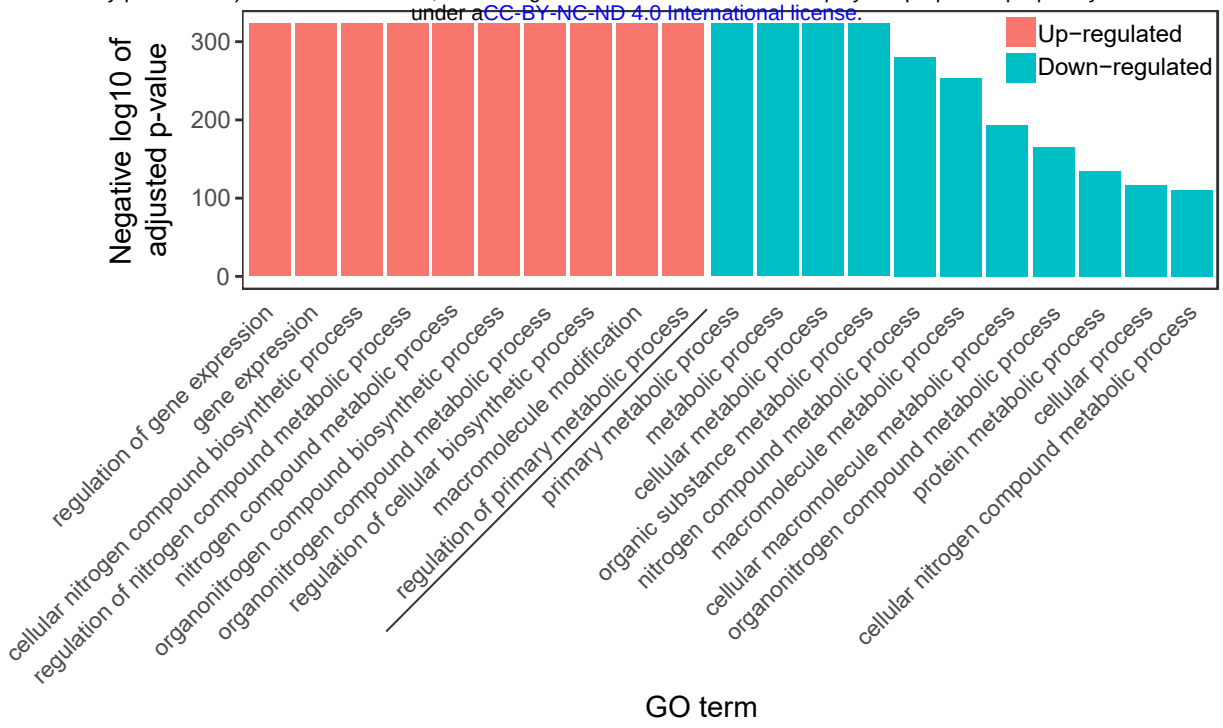

Figure 5. GO enrichment analysis for top Biological process GO terms with the highest p-value for up- and down-regulated genes in the sample group with a candidate seminal root angle QTL compared to without the QTL.

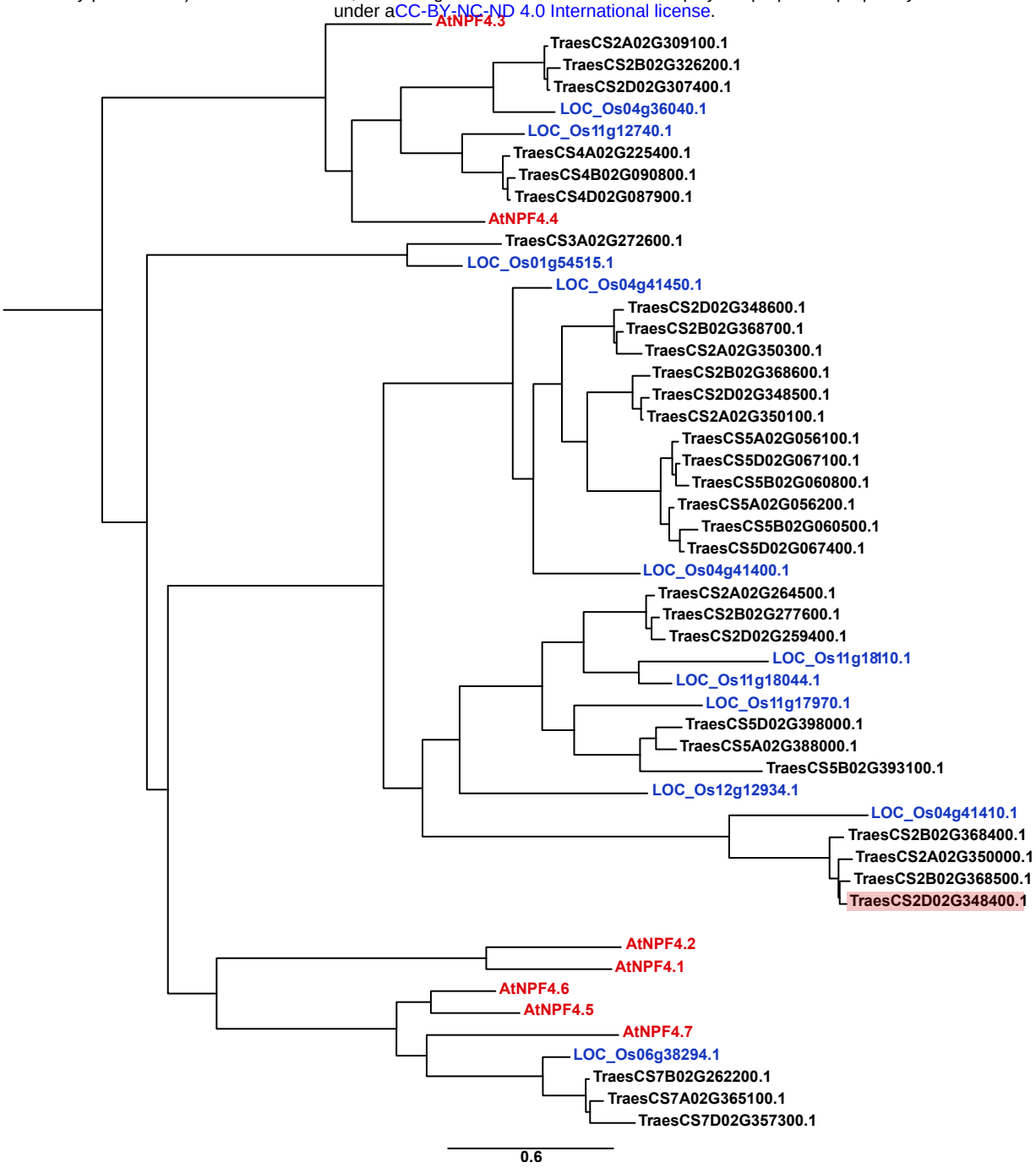

Figure 6. Phylogenetic tree of protein families comparing the protein sequences of A. thaliana, O. sativa L. and T. aestivum L. NPF family proteins to an identified candidate T. aestivum. protein. The candidate T. aestivum. protein is situated in a monocot specific outgroup within a NPF4 protein clade (highlighted in red). Branch lengths are proportional to substitution rate.